

Design of pulse power supply for klystron and its noise characterization

Sandeep Kumar R*, Kiran Thakur* and Krishnan R*

At SAMEER, extensive developments are being carried out in the field of high energy electron linear accelerator technology primarily for medical applications. In linacs, electrons are accelerated to fractions of light speed and such energy is derived through interaction with high power microwaves generated by Klystron in a specialized accelerating structure. These high power RF klystrons employed as RF amplifier in turn derive this energy from high voltage pulsed dc power supply commonly called as Modulator. Currently, we have our expertise in development of 15 MV linear accelerators which requires a 6 MW high power RF Klystron. The pulse generator driving this Klystron has maximum peak power rating of 14.4 MW; average power rating of 14.68 kW and discharges 74.59 Joules of energy into the Klystron tube during each pulse.

High power pulse generator employs line type topology i.e., an E-type PFN is used as lumped equivalent of transmission line to generate the desired pulse width of 6 μ s. The energy stored in PFN is discharged using a high voltage switch namely, Thyatron. This high voltage switching produces a large transient noise that is coupled with many other local electronic circuits. Apart from thyatron there are many other sources that may generate noise, so a study has been carried out to identify the noise sources in pulse generator in which exhaustive data has been collected and analyzed. This paper provides the design of discharge section of power pulse generator, data acquisition setup, noise waveforms at different locations of modulator and the interpretation of data in identifying the problem posed by high voltage systems on low voltage control systems.

Keywords: Thyatron, klystron, pulse power system, pulse forming network.

1.0 INTRODUCTION

PULSED power science and technology deals with physical and technical foundations for production and application of high voltages pulses with very high peak powers. It includes transformation of electrical energy into high accumulating energy over a relatively longer duration of time and then releasing it in a shorter duration thus increasing the instantaneous peak power levels in association with the compression of time duration [1, 2]. There has been a great transformation in the pulsed power sources from the natural ways (Clouds) to

radar power supplies during World War II [3] and further to many diversified applications namely particle beam diodes, plasma, biological samples, defence, environmental and biomedical applications in the present day [1-14]. Now a day's pulsed power technology has novel applications namely electric discharge food processing technology [4, 12] for microbial inactivation, concrete waste management technology [5], generation of non-thermal plasma that has the ability to attack biological and chemical agents and is in particular promising for decontamination and purification of water [11] and also in cutting edge applications

such as the generation of X-rays [6] and high power microwaves [7]. It is used in pulsed high power laser systems, and also the generation of shockwaves to dissolve kidney stones (lithotripsy) [8].

It is a unique way to generate dense plasmas in plasma focus [9], and also produces a burst of neutrons, which can be used for detection of explosives and illicit materials [10]. A growing interest in pulsed power technologies can also be found for industrial, medical, biological and environmental applications. Electro-mechanical forming and Electro-hydro forming are techniques for welding or cutting the materials at high velocity [1]. Another emerging application is the manipulation of mammalian cells with pulsed electric fields [13-14].

At SAMEER, pulsed power technology is a part of the linear accelerator development for major biomedical applications like Radiotherapy and Radio isotope generation. Our linacs are operated in S-Band at operating frequency of 2998 MHz and presently developing modern high energy linac which will provide two photon energies (6 and 18 MV) and several electron energies (6, 9, 12 and 18 MeV). The intersecting area of these fields is generation of high energy Bremstrahlung X-rays [15-16] which requires a high power microwave sources like Klystron operating in pulse mode [17-19]. A pulse power supply is used to provide the high voltage biasing pulses necessary for the amplification of RF power to peak powers [17] of up to 6 MW. These microwave power sources have very specific pulse power requirements namely the flat top ripple, shape rise times and fall times etc., which demands very specific design considerations in the generation of high voltage pulse [17]. Also, for applications like generation of radio isotopes along with high peak pulse power high average power is required. The trend in repetitive pulse power system design is toward higher energies, larger average power levels, and faster pulse repetition rates; thereby increases the design issues in terms of high voltage switch,

heat considerations, de-rating of components, transient noise and EMI/EMC.

Development of pulsed power supply is very critical, expensive and important in pulse related applications. Keeping in view the criticality of end user application i.e. treatment of cancer patients, it has been proposed to review the design of power pulse generator and assure the quality of each component used in the system. This would also help to detect any worst case failures that may occur in the linac and provide an anticipatory solution. As a part of proposed work, authors performed the noise characterization of pulse generator by monitoring, acquiring and analyzing the degradation of signals at different points in the supply. Generally electronic systems involving components requiring DC power supply employ ac to dc conversion circuits in power supply which are figured out to be one of the largest sources of EMI [20-21]. The unwanted high frequencies created by these power supplies may not affect the functional operation of electronic product except coupling back to the product's AC power cord. It is to be emphasized that this is not same in the case of high voltage pulse generator employed in Linear Accelerators. These unwanted frequencies do affect the functional operation of control circuitry and may at times lead to fatal problems and also importantly makes it a very tough to pass the regulatory test.

Present paper discusses the design of discharge section of pulse modulator, reports the observed noise signals and discusses their probable origin. A complete analysis of these noise frequencies is carried out to understand the problems associated with transient noise and EMI/EMC noise independently.

2.0 DESCRIPTION AND DESIGN OF SYSTEM

This section presents the description of system and design of pulse generator to accommodate with the specifications of Klystron.

2.1 Block Diagram of linac and Modulator

A simplified block diagram of linac System is shown in Figure 1. In basic terms, an RF linac uses electromagnetic energy of high power in microwave region to create electric fields so as to accelerate electrons in specially designed structures. The accelerated electrons whose speeds are fractions of light speed strike a metal target to produce X-rays. The high voltage bias pulses required to operate microwave generators (namely Klystrons and Magnetrons) are generated by a power pulse generator commonly called as “Modulator”. Modulator provides voltage pulses of 12 kV with duration of 6 μ s capable of sourcing a current of 1078 A when applied across an equivalent load of Klystron as seen from primary of the pulse transformer of Turns Ratio 1:11 i.e. 12.25 Ω with repetition rates ranging from 20 Hz to 170 Hz. A pulse forming network (PFN) comprising six LC stages is charged through a high DC voltage source via a charging choke. The high DC voltage of 12 kV is generated by six-phase rectification of stepped-up 3-phase AC input voltage. The topology of Modulator being implemented is conventional Line-Type Modulator [18] which employs DC sub-resonant mode of charging a pulse forming network (PFN). The PFN is discharged through a high voltage switch namely thyatron to the primary of the pulse transformer. Figure 2 shows the block diagram of pulse modulator. Pulsed power system is specified by the power levels delivered to the load (Klystron), energy stored in the system, duration of the pulse, number of times the pulses are repeated and size of the energy storage medium. Table 1 and 2 provides the specifications of Klystron load and the specifications of pulse power supply.

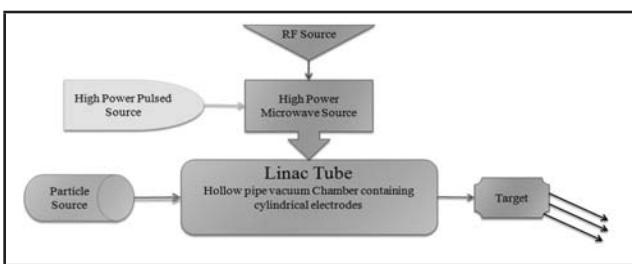


FIG. 1 BLOCK DIAGRAM OF LINEAR ACCELERATOR

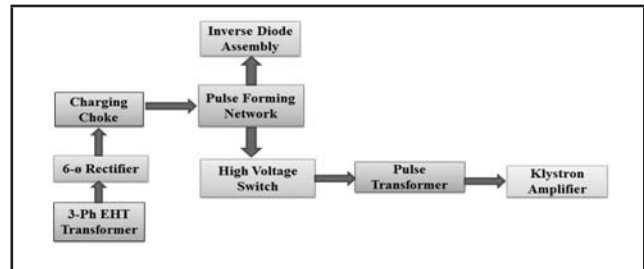


FIG. 2 BLOCK DIAGRAM OF PULSE POWER SUPPLY FOR KLYSTRON

TABLE 1
SPECIFICATIONS OF VKS8262H KLYSTRON

Parameter	Operating	Maximum
Peak RF Power(MW)	6.0	6.15
Frequency(GHz)	2.998	2.998
Beam Voltage(kV)	132	135
Cathode Current(A)	98	109
Gain(dB)	48.4	48.4
RF Input Power(W)	87	135
Perveance	1.94E-6	1.94E-6
PRF(Hz)	170	305
Avg. RF Power(kW)	6.12	15.6
PulseWidthtp(RF)(μ s)	6.0	8.5
Duty Cycle(RF)	0.001	0.0026

TABLE 2
SPECIFICATIONS OF PULSE POWER SUPPLY

Energy	75 J
Power	11.76 MW
Voltage	12 kV @ Primary of PT
	132 kV @ Secondary of PT
Current	1078 A in primary
	98 A in secondary
Pulse Width	6 ms(fixed)

2.2 Design Of Discharge Section

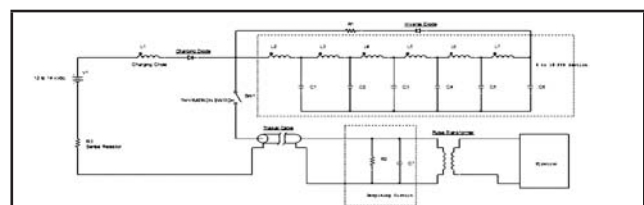


FIG. 3. CIRCUIT DIAGRAM OF POWER PULSE GENERATOR

The specifications in Table 2 details out the necessary parameters that are to be considered while designing the high power pulse generator.

The main specification is the pulse length i.e. $6\mu s$, correspondingly this short pulse give approximate peak power multiplication 10^3 times of the average power. The topology of the pulse power circuit is shown in Figure 3. It shows a cascaded network of inductors and capacitors namely pulse forming network (PFN E-type) which is the lumped version of a transmission line. The transmission line circuits offer the possibility of realizing fast rectangular pulses while connecting energy storage elements to loads. The generation high voltage pulse is accomplished by the pulse-forming network (PFN) charged to 24 kV and discharged through a thyatron (CX1559) and pulse transformer. The high power pulse is generated is characterized by its shape, flatness of its plateau region. The fall time of pulse depends on the evolution of the load impedance. The pulse transformer used is SI 16990 manufactured by Stangenes with turns ratio 1:11.

$$\begin{aligned} & \text{Impedance of Klystron } (Z_{kly}) \\ & = \frac{\text{Peak Beam Voltage of Klystron}(V_{kly})}{\text{Cathode Current}(I_{kly})} = 1346.9 \Omega \end{aligned}$$

Reflected Impedance of Klystron at primary of the pulse transformer:

$$Z_{ref-kly} = \frac{\text{Impedance of Klystron}(Z_{kly})}{11 * 11} = 11.13 \Omega$$

The percentage of negative mismatch is chosen as 10 %. From the above calculation a PFN has to be designed that has characteristic impedance as 12.25 ohms and propagation delay of $6 \mu s$. The Peak pulse voltage at the primary of the pulse transformer is the output of Line type Modulator.

$$\begin{aligned} & V_{peak-pri} = V_{peak-Mod} \\ & = \frac{\text{Peak Beam Voltage of Klystron}(V_{kly})}{\text{Turns Ratio}} = 12.0 kV \end{aligned}$$

The peak pulse current through primary of the pulse transformer:

$$\begin{aligned} & I_{peak-pri} = I_{peak-Mod} \\ & = \text{Peak Beam Current of Klystron}(I_{kly}) * \text{Turns Ratio} \\ & = 1078 A \end{aligned}$$

The peak pulse power of Modulator:

$$P_{peak-Mod} = V_{peak-Mod} * I_{peak-Mod} = 12.9 MW$$

The average power given out by modulator:

$$\begin{aligned} & P_{Avg-Mod} = P_{peak-Mod} * T_p * PRF \\ & = 12.9 MW * 6\mu s * 170Hz = 13.19 kW \end{aligned}$$

For any transmission line when connected across a matched load, as per maximum power transfer theorem the voltage at the load gets half of the input voltage. So the PFN is to be charged to a voltage which is twice that of the peak pulse voltage.

Peak DC charging voltage on PFN

$$V_{dc-PFN} = 2 * V_{peak-Mod} = 24.0 kV$$

A PFN is to be designed with a characteristic impedance of 12.25Ω (considering the negative mismatch of 10%) and propagation time of $6\mu s$. Characteristic Impedance and the pulse width can also be represented using total inductance and capacitance value of the PFN as follows:

$$Z_{pfn} = \sqrt{\frac{L_n}{C_n}} \quad \begin{aligned} L_n &= \text{Total inductance of PFN} \\ C_n &= \text{Total capacitance of PFN} \end{aligned}$$

$$T_p = 2 * \sqrt{L_n * C_n}$$

$$C_n = \frac{T}{2 * Z_{pfn}} = 0.245 \mu F$$

$$L_n = \frac{Z_{pfn} * T}{2} = 37.5 \mu H$$

The capacitor with a capacitance of $0.047 \mu F$ is chosen and it can be used to determine the number of sections of PFN.

$$\begin{aligned} & = \frac{\text{Total Capacitance of PFN}(C_{PFN})}{C_{each}} \\ & = \sim 6 \text{ sections} \end{aligned}$$

The average current through high voltage switch is calculated as:

$$\begin{aligned} I_{avg-Mod} &= I_{peak-Mod} * T_p * PRF (\text{Max}) \\ &= 1.10 A \end{aligned}$$

2.3 Results

From the above calculations, a PFN of 8 sections and 6 sections is simulated in Pspice to generate 8 μ s and 6 μ s pulses respectively. The E-type PFN has continuous solenoid with tapings at each section and this provides mutual inductance effect modifying the network inductance. This mutual inductance is represented by coupled inductors in Pspice simulation. An important requirement of voltage pulse is the flattop ripple, as the variation in applied voltage to RF source causes variation in electron velocity further implies variation in electron transit time. This in turn changes the arrival time at gap of the output cavity in Klystron. Overall this causes variation in phase of the output microwave and the variations in the final dose output of the linac. So PFN is modelled for the ripple of 2 to 3 % and the values of mutual inductances are defined. Figure 4 shows the PFN and Figure 5 & 6 show simulated pulse of 8 μ s and 6 μ s pulse for the measured value of inductance with ripple of 2 to 3 %. Table 3 shows the specifications of the pulse. Figure 7 shows the developed Modulator and Figure 8 shows the Klystron voltage and current waveforms.

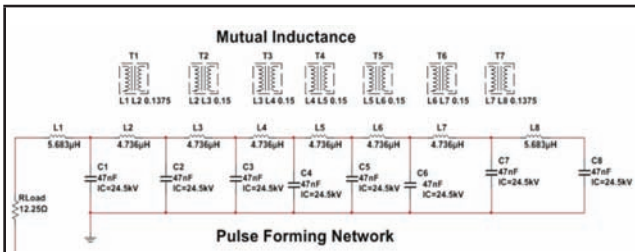


FIG. 4. 8 SECTIONS PFN MODELLED IN PSPICE ALONG WITH MUTUAL INDUCTANCES

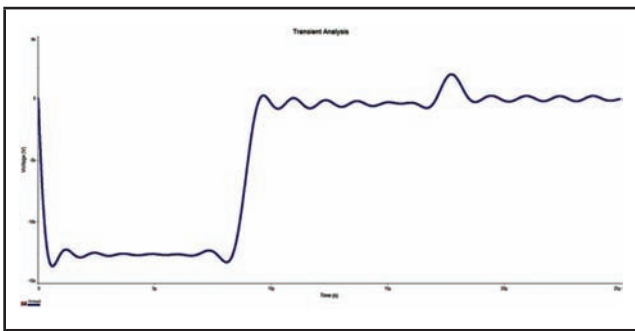


FIG 5. SIMULATED PFN PULSE OF 8 US

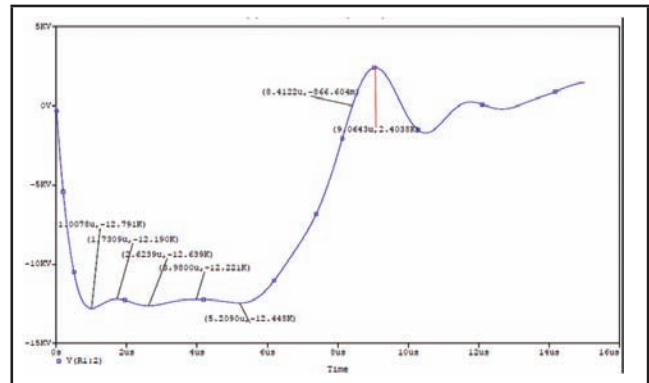


FIG 6. SIMULATED PFN PULSE OF 6 US WITH MEASURED INDUCTANCE VALUES

Parameter	Simulated	Experimental
Pulse Voltage	11.62 kV	11.8 kV
Rise time	451.3 ns	700 ns
Fall time	451.3 ns	1500 ns
Inverse Voltage	1.7 kV	2.40 kV
Pulse width (50%)	8.78 μ s	5.8 us
Ripple in flat top	± 1 %	± 2 %

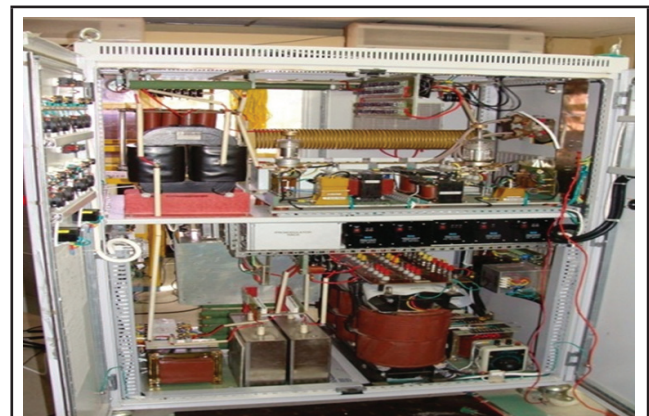


FIG 7. 14.4 MW PEAK POWER PULSE POWER SUPPLY FOR VKS8262H

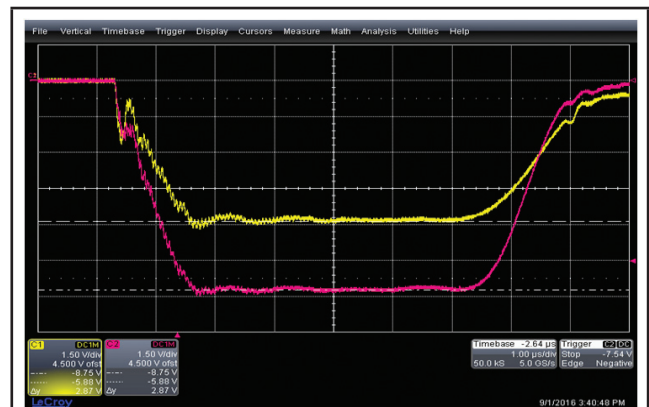


FIG 8. VOLTAGE AND CURRENT WAVEFORMS AT THE KLYSTRON END WITH THE IMPLEMENTED PFN

3.0 NOISE CHARACTERIZATION OF MODUALTOR

SAMEER has its expertise in development of lower energy 6 MV medical linear accelerators, a few of which have been successfully installed in cancer treatment hospitals in India. Recently we proposed the development of high energy linear accelerator i.e., 15 MV dual mode multi energy system. We have adopted the same Modulator topology with necessary changes to adhere the need of high peak and average powers for the high energy modulator. During the in-house testing of linac we have observed frequent failures of the system, random flickering or triggering of pseudo faults and also blew the FPGA based controller. The preliminary measurement of CISPR 11 for CE test also failed. Even though no such serious issues were reported with our installed lower energy systems, at times there was sudden breakdowns due to unidentified reasons.

In order to address these issues it was proposed to characterize the modulator in terms of noise since it is the power source of linac. A test setup with all the systems has been made along with high end data acquisition systems with interactive automated graphical user interfaces. Also many test benches were built during this work to test the behaviour of individual components used in Modulator. The methodology adopted is to observe the signals at different locations of modulator during operation, acquire and extract the frequency information from these signals. The trend of these noise frequencies is observed with respect to increase in pulse voltage and pulse repetition frequency. Further the monitoring points are mapped as per the noise coupled or generated. This would help us to understand the type of noise generated and its propagation into the subsystems attached. The major results are being reported here.

3.1 Power Quality and Inrush Measurements

For an electrical system involving three phase input, monitoring the line voltages and line currents provide a great deal of information

about the device in use which acts as load. So line voltages and line currents have been acquired. Figure 9 shows the line currents and neutral current acquired by using power quality analyser. This preliminary results show that the load distribution on three phases is not equal and unbalanced. Also, great amount of distortion can be observed in line currents due to harmonics generated by six-phase rectifier circuit, pulsed operation of modulator and other non-linear loads attached. It has been noted that at times there was frequent tripping of the circuit breaker at the moment three phase supply is connected to the transformer for high voltage DC generation. It was thought that this might be due to high value of inrush currents generated due to the capacitor attached to the rectifier circuit. Figure 10 shows the observed inrush currents of 800 A when switched on at full load. It was observed that the value of inrush current was same even for no-tripping condition. Later it was concluded that the tripping is due to the time at which contactor is closed which would have same magnitude but different signal shape which will be sensed by the circuit breaker as fault occurrence. It was further proposed to use a power factor correction circuit at the input lines.

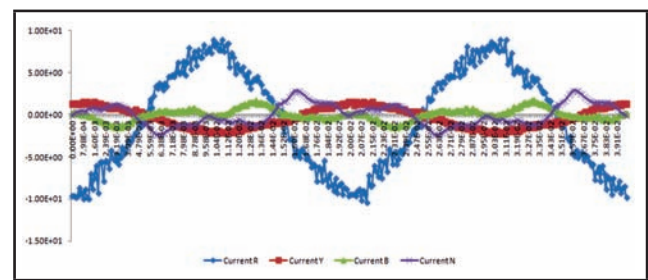


FIG. 9. LINE AND NEUTRAL CURRENTS DURING OPERATION

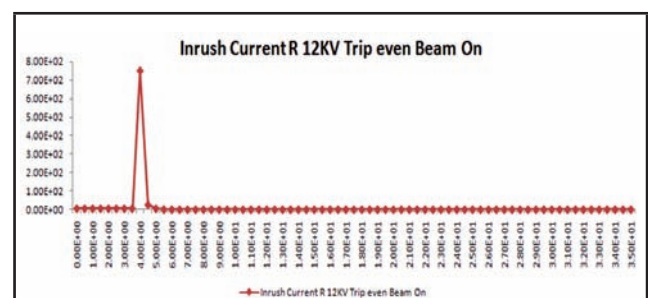


FIG.10. INRUSH MEASUREMENTS ON THE INPUT AC LINE

3.2 Harmonic Analysis

Harmonics in a rectifier based circuit are common but are unintended and could affect the operation of the overall system. It is necessary to study the extent and propagation of these harmonics in the pulse modulator as they are comparable to Pulse Repetition Frequencies (PRF) employed. In a nut shell it can be stated that if the harmonics propagation is not estimated properly then there is every chance of these frequencies interacting with a subsystem circuitry that work in the mentioned PRF (10 Hz to 300 Hz) range. As a part of this work harmonics at different locations are acquired and observed an unintended change in amplitudes at power line filter which is in the path of three phase supply to high voltage transformer. The results are shown in Figure 11. The plots show the frequency components greater than 100 Hz excluding the component of fundamental or mains frequency (50 Hz) on L2(Yellow) line and Neutral. It can be inferred from the above results that frequencies above 3rd harmonic i.e.150 Hz, 5th Harmonic i.e., 250 Hz, 7th Harmonic i.e., 350 Hz and so on increases in amplitude after passing through line filter.

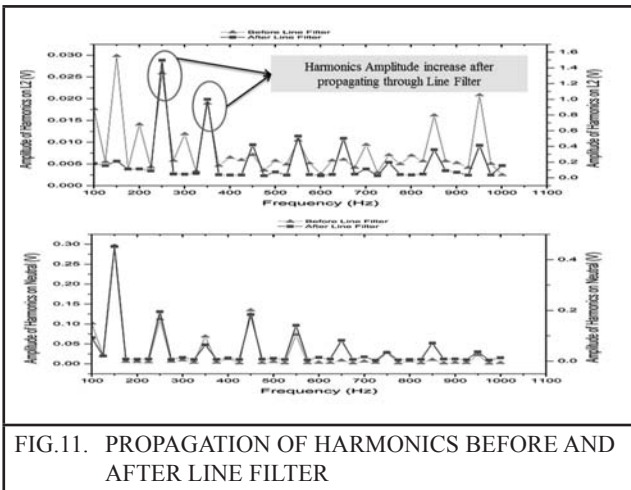


FIG.11. PROPAGATION OF HARMONICS BEFORE AND AFTER LINE FILTER

3.3 Line Filter Characterization

In order to explain the reasons for this anomalous behaviour of line filter at harmonic frequency range it became necessary to characterize it over broad range of frequencies other than the EMI frequencies (150 kHz to 30 MHz). General parameter to characterize the functional

behaviour of line filter in estimating suppressing effectiveness is Insertion Loss (I.L). It is defined as ratio of voltage $V_{L\omega 0}$ across the load impedance without filter and $V_{L\omega}$ across the load with filter as given in equation (1). The components of line filter along with their connections for single phase are shown in Figure 12. The values of the components shown are taken from the data sheet [25-26]. Available literature details the effect of variation in source and load impedances of line filter but all studies are restricted to EMI frequency band only i.e. 150 kHz to 30 MHz. Based on the results shown in Figure 11 the response of the filter over frequencies other than EMI band may pose undesirable effects on the electronic system. We characterized line filter using frequency response analysis (FRA) technique for the case of “matched” load $50\Omega/50\Omega$ over frequency range of 10 Hz to 100 MHz. Power line filter can best be type casted as a Low Pass Filter (LPF), so as to determine cut-off frequency of the filter, circuit shown in Figure 12 is analysed using concepts of network theory. Upon simplification with the above mentioned component values and by neglecting the lowest value coefficients Insertion Loss (I.L) can be deduced as shown in equation (3).

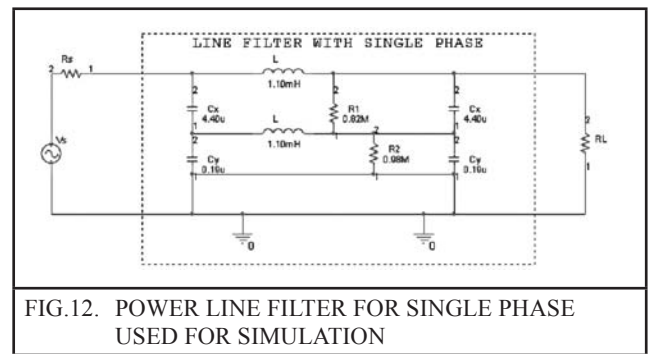


FIG.12. POWER LINE FILTER FOR SINGLE PHASE USED FOR SIMULATION

$$Insertion Loss(IL_{dB}) = 20\log_{10}\left(\frac{V_{L\omega 0}}{V_{L\omega}}\right) \quad \dots(1)$$

Where $V_{L\omega 0}$ Voltage across load resistor (R_L) with no filter; $V_{L\omega}$ Voltage across load resistor (R_L) with filter;

$$Insertion Loss(IL_{dB}) = 40\log_{10}\left(\frac{144736}{\omega}\right); \quad \dots(2)$$

$$Insertion Loss(IL_{dB}) = 206.4 - 40\log_{10}(\omega); \quad \dots(3)$$

Where $\omega=2\pi f$; f= frequency

To determine the cut off frequency i.e. the frequency below which no attenuation is experienced from input port to output port, equation (3) is solved by perpendending zero Insertion Loss (I.L). It is enciphered that for all frequencies greater than 23 kHz; Insertion loss is greater than 0 dB i.e. the signal at input port gets attenuated and is not transmitted to output port. For all frequencies less than 23 kHz; Insertion Loss is less than 0 dB i.e. the signal from input port gets completely transmitted to output port. The practical filter might not have such a sharp response and the simulated frequency response of circuit shown in Figure 12 using Orcad (Pspice) is shown in Figure 13. The cut-off frequency derived from the simulated response is 19.14 kHz is in close agreement with the calculated value. The simulated response of line filter befits to the response of a practical low pass filter but an unanticipated peak is observed near the cut-off frequency necessitates obvious reasoning. This increase in gain of the line filter around cut-off frequency is caused due to the resonance of inductor and capacitor i.e. resonant peak observed at around 10 kHz frequency. Further the above simulated response of the filter is verified with an experimental setup.

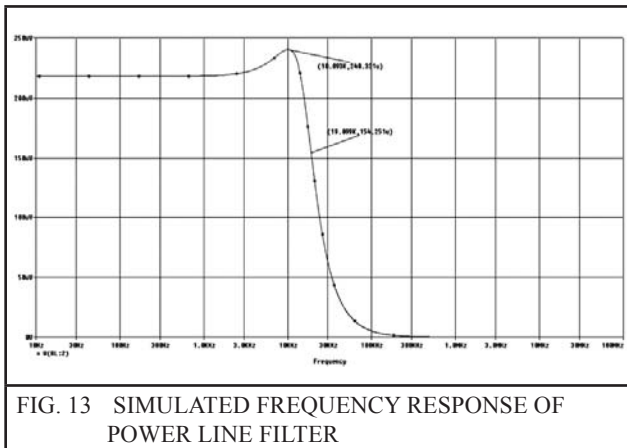


FIG. 13 SIMULATED FREQUENCY RESPONSE OF POWER LINE FILTER

The experimental setup for characterizing line filter over the desired frequency range of 10 Hz to 100 MHz employs an Arbitrary Function Generator, Tektronix Digital Storage Oscilloscope and PC with LabVIEW Software. A sine wave of $4 V_{p-p}$ is generated by the AFG, the frequency of the sine wave is swept over the range of 10 Hz to 100 MHz and is applied to the input port of line filter in common mode configuration. The control

and data acquisition GUI sets the frequency of AFG and commands DSO to acquire the signals at the input as well as output averaged over 60 sweeps thus providing more stable peak to peak measurements. Further V_{p-p} of input and output signal is measured, recorded and tabulated for the corresponding frequency. The above steps are repeated for the required range of frequencies by the automated sweep function embedded in the GUI. The tabulated data is plotted and is shown in Figure 14.

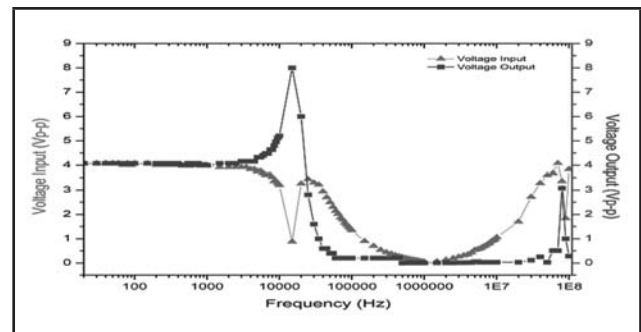


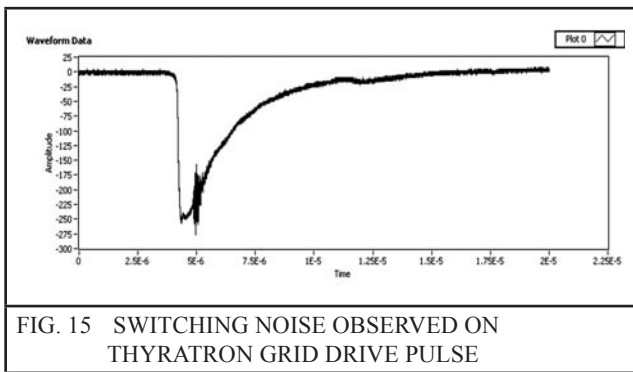
FIG. 14 FREQUENCY RESPONSE OF LINE FILTER OVER FREQUENCY RANGE 10 HZ TO 100 MHZ (EXPERIMENTAL)

The trend of the output voltage response is in complete accordance with the simulated result. It can be deduced from the plot that for frequencies less than 1 kHz i.e. in passband frequency range the output voltage measured is more than input voltage. The difference in input and output voltage further increases with increase in input voltage and is accountable for increase in harmonics amplitude after passing through line filter as shown in Figure 11. The cut-off frequency is measured to be around 20 kHz and the frequency at which resonant peak is observed is 15 kHz. The slight deviation of resonant peak frequency from that of simulation may be associated to non-consideration of lead inductances and stray capacitances.

Authors would like to emphasize here that for a system as linac comprising power devices and circuits viz. the power pulse generator, the above shown characteristic of line filter may affect the operation of other subsystems like controls, low voltage circuitry etc. In a more detailed way, power pulse generator is a source of huge transients and impulses of broadband frequency comparatively

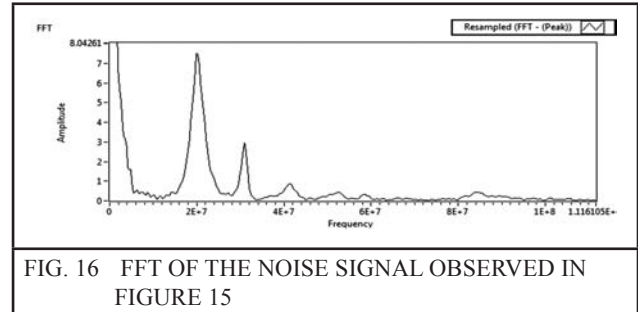
with high voltages. Any subsystem or device in their path tends to resonate thus transferring the energy. Similarly line filter would resonate around the frequency of resonant peak, passes them through with increasing amplitudes. When this signal attains appreciable voltage level, it will always interact with the other electronic circuits, subsystems leading to their failure or impressing errors in communication or evoking of pseudo alarms. Thus a power line filter may provide better performance in EMI range nevertheless it is quite important to observe its response in the other frequency range too.

3.4 Thyatron Noise Effect on Modulator Control Circuitry

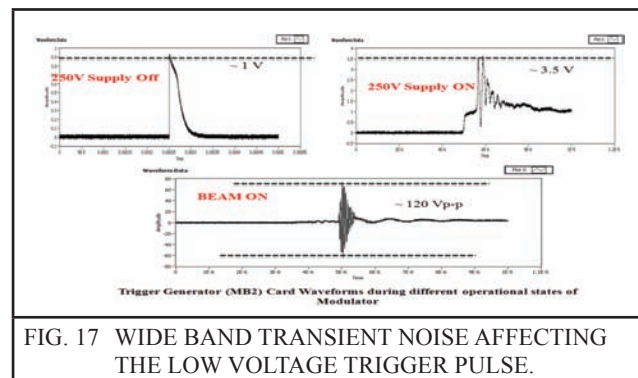


Discharge circuit presented in section 2 is the main source of noise in the pulse modulator of linac. It consists of PFN, high voltage switches (Thyratron), pulse transformer and pulse transmission cable. Upon switching thyatron of pulse modulator the energy stored in PFN capacitors is discharged into the klystron through pulse transformer. The two main sources of noise in discharge section are thyatron switching and loop current from PFN to klystron which mainly depends on the rise time of the high voltage pulse [22-24]. Reference [23] explains the processes underlying in generating the noise by the above mentioned sources and their ways to couple with other systems. The frequency of noise generated by thyatron switching is in the range 10 MHz to 100 MHz. A frequency of 30 MHz is reported [22], which is proportional to the transit time of ions generated in plasma and has wider frequency spectrum. Figure 15 shows the coupled thyatron

noise on its grid driving pulse signal of amplitude -250 V and its FFT is shown in Figure 16. The maximum frequency of noise is 20 MHz and also includes 32 MHz, 42 MHz, other frequencies have negligible amplitudes.



To further observe coupling effect of this noise with other systems the low voltage SCR trigger pulse that is supposed to fire 250 V is monitored and recorded at different operating instances of the system as shown in Figure 17. It had been observed that during the full voltage operation ratings of Modulator the noise on the low voltage trigger signal would reach to a level of 200 Vp-p completely masking the trigger signal of 1 V. Figure 18 shows the frequency spectrum of this noise and is understood that this circuit is resonating with the 20 MHz frequency component of thyatron noise. Such huge levels of noise not only degrade the EMI/EMC performance but also would become the unidentified reasons accounting for components and system failure. Figure 19 shows the voltage and current pulses of the pulse modulator with resistive load along with noise on timing signal and low voltage SCR trigger signal. The noise is coincidental with the firing of thyatron and can be concluded as major noise source.



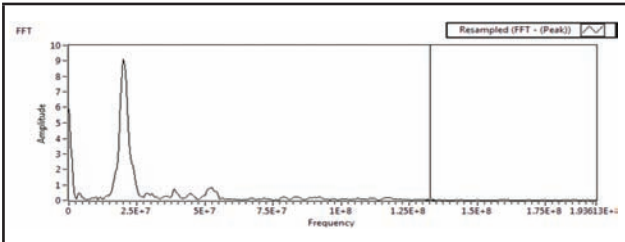


FIG. 18 FREQUENCY SPECTRUM OF THE NOISE SIGNAL IN FIGURE 17

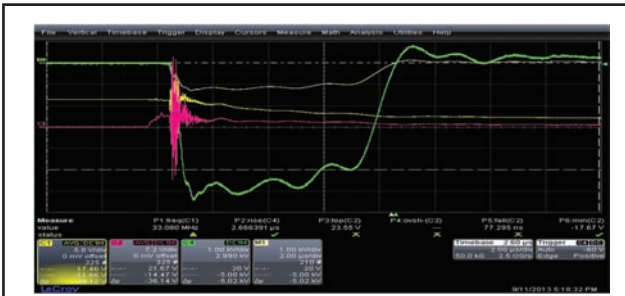


FIG. 19 VOLTAGE AND CURRENT PULSES OF THE PULSE MODULATOR WITH RESISTIVE LOAD ALONG WITH NOISE ON TIMING SIGNAL AND LOW VOLTAGE SCR TRIGGER SIGNAL

3.5 Impact on AC line VOLTAGES, Klystron and Control Console

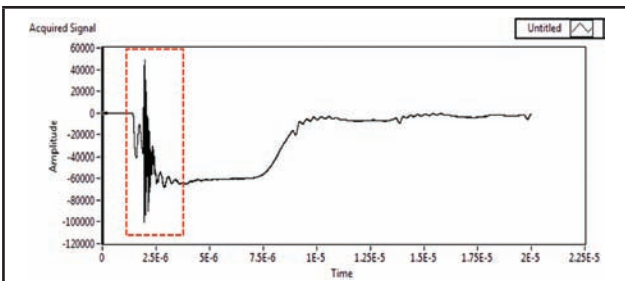


FIG.20 NOISE COUPLED ON KLYSTRON VOLTAGE WAVEFORM

The thyatron noise which has broad frequency spectrum couples with all other subsystems and circuits attached to linac at their own resonant frequencies affecting and interfere their normal operation. Figure 20 shows the noise coupled on klystron voltage waveform that is being sensed by a high voltage CVD probe. Figure 21 shows the same thyatron noise on the AC line waveform. It was proposed to fully test the FPGA based computerized control console so as to find out the impact of such high noise environment on the sensitive controller and also determine the reasons for failure of the ADCs, unreliable operation of console etc. The pattern and levels

of noise reaching control console that may force it to malfunction are exhaustively monitored. Figure 22 shows the on the 24 VDC logic lines and ADC lines of the control console.

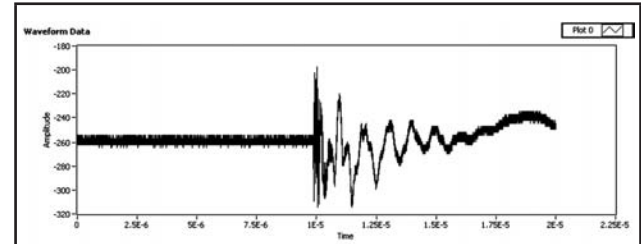


FIG. 21 THYRATRON SWITCHING NOISE ON THE AC LINE WAVEFORM

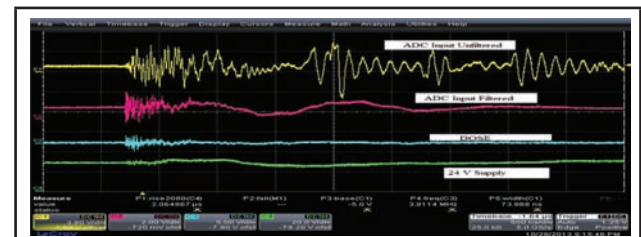


FIG.22 NOISE COUPLED ON 24 VDC LOGIC LINES AND ADC LINES OF THE CONTROL CONSOLE.

In order to compare and visualise complete range of noise emanated these waveforms are observed with three different PRFs and at voltages from 0 kV to 12 kV in steps of 2 kV. The three PRFs selected are 30 Hz, 80 Hz and 130 Hz. The pattern of noise observed at the ADC input is comprised of Differential (random) and Common mode (periodic). So the analysis for the ADC unfiltered input is divided into two sections i.e., independently for differential noise at the start of the waveform and common mode noise in later time by extracting all the frequency components using the user interface developed in LabVIEW. Figure 23 shows the variation of the noise frequencies for the first section of unfiltered ADC signal with increase in the voltage and repetition frequency of the modulator.

At all PRFs and voltage levels the observed noise frequency range is 1 MHz to 100 MHz, of which components of 8 MHz and 32 MHz are significant. The band of noise from these frequencies may be attributed to 5 to 45 MHz. All the frequency components increase with respect to KV with slightly non-linear nature. The two frequency components of 8 MHz and 32

MHz are significant. It can be observed that even though there is an increasing trend with respect to pulse voltage level, there is a shift in noise level after 6 kV. From this it can be concluded that controller circuits for higher energy linacs(15 MV) systems require to have more immunity in terms of noise compared to lower energy (6 MV) medical linacs.

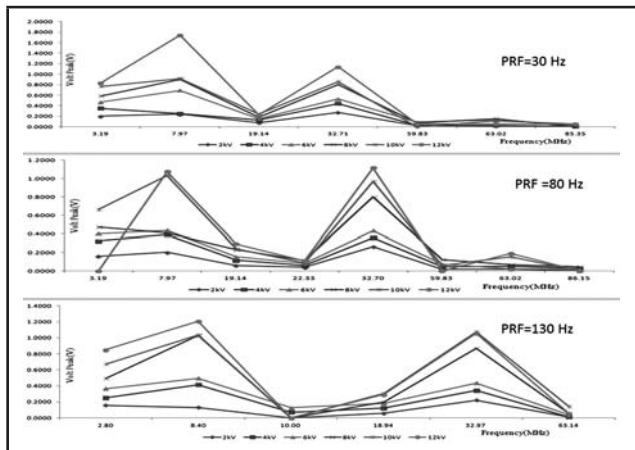


FIG. 23 VARIATIONS OF THE NOISE FREQUENCIES FOR THE FIRST SECTION OF UNFILTERED ADC SIGNAL WITH INCREASE IN THE VOLTAGE AND REPETITION FREQUENCY OF THE HIGH POWER PULSE GENERATOR

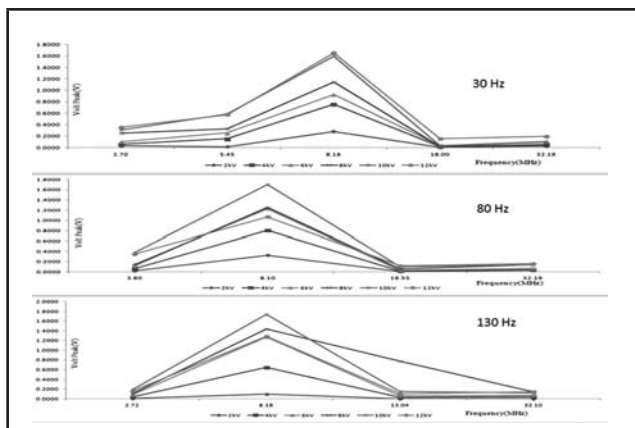


FIG. 24 VARIATIONS OF THE NOISE FREQUENCIES FOR THE SECOND SECTION OF UNFILTERED ADC SIGNAL WITH INCREASE IN THE VOLTAGE AND REPETITION FREQUENCY OF THE HIGH POWER PULSE GENERATOR

Figure 24 shows the variation of the noise frequencies for the second section of unfiltered ADC signal with increase in the voltage and repetition frequency of the high power pulse generator. The major frequency component is 8 MHz which is mostly common mode noise frequency component. The first section of the

signal is combination of both differential and common mode noise and is verified from the observation of 8 MHz frequency component which was mostly following irregular trend from the analysis of first section of the waveform. It is understood that due to these noise pickups dosimeter circuit measures errant values which increases with respect to PRF and kV clearly agreeing with the increasing trend of noise.

4.0 CE TEST ON MODULATOR

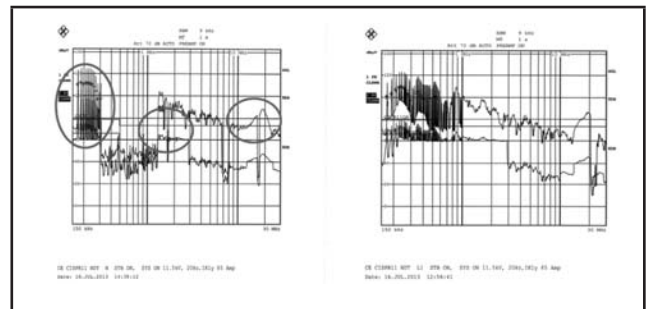


FIG. 25 CONDUCTED EMISSION (CE) RESULTS MEASURED AT FULL VOLTAGE OPERATION WITH REPETITION FREQUENCY OF 20 HZ

A comparative study is done on the results of noise characterization and Conducted Emission (CE) regulatory test (CISPR 11) performed on the high power pulse generator. Figure 25 shows the Conducted Emission (CE) results measured at full voltage operation with repetition frequency of 20 Hz. The observed frequency range of noise from the CISPR 11 test confines mostly to the band of 200 KHz to 3 MHz and greater than 20 MHz but the frequencies mentioned from the analysis carried out agree at higher frequencies i.e., 3 MHz and 20 MHz with that of CISPR 11 test but the frequencies mentioned from the analysis carried out are slightly different from that of EMI/EMC report. The difference can be attributed to the measuring techniques i.e. Quasipeak detection method used by EMI receiver that reports frequency components with weight proportional to the occurrence of particular component during large monitoring time duration. Since the transient noise discussed here is present only at the time of triggering which is equal PRF that makes it insignificant in the CE test where as DSO employs trigger based acquisition that reports good information about the transient noise frequencies. This data is in good agreement with

the results derived using our non-conventional lab setup and validates the measurement methodology and it can be inferred from the EMI/EMC report, common frequency components like 3 MHz and 20 MHz are significant.

5.0 REMEDIAL MEASURES

This complete picture of noise and its propagation is used in immunizing control console by designing filters, transient suppressors and isolators. Even though noise is not reduced at source the immunizing methods used in control console ensured hassle free operation by hindering its propagation. Further each subsystem discussed above is addressed and remedies have been worked out to modify them for better noise performance.

Power line filter’s resonance peak effect is reduced with the help of cascading filters. EMI filters are cascaded with another class of filters that work in low frequency range and reduce the effect of resonant rise. A simpler of such cascading filters is RC-Shunt filter with a capacitor and a series resistance. This requires fewer components and is automatically balanced across the line. The cut-off frequency of this RC-Shunt filter is chosen as 15 kHz derived from the plot shown in Figure 14 and the design impedance is calculated by dividing the highest current required by the load to the lowest anticipated line voltage, corresponding to a series resistor value of 10 Ω and capacitor value is calculated to be 1 μf. The RC-shunt filter is added in series with the line filter. The voltage response of the cascaded filter with frequency is shown in Figure 26.

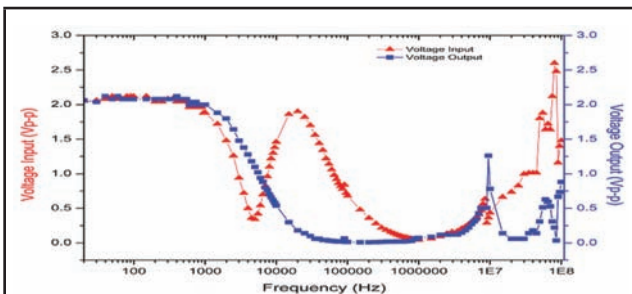


FIG. 26 FREQUENCY RESPONSE OF THE CASCADED FILTER

Further the coupling of wide band noise on the low voltage trigger pulse is reduced by employing fiber optic transmission of pulse from controller to the power switch. The block diagram of the circuit topology is shown in Figure 27. This provided better isolation and noise performance. There is still some noise coupling as shown in Figure 28 but it is extremely weak in terms of amplitude. The noise frequency on the trigger line is now narrow band in the frequency range 18 MHz to 24 MHz and the peak amplitude of maximum noise frequency is 0.5 V which is greatly reduced compared to the previous value of 9 V as shown in Figure 28.

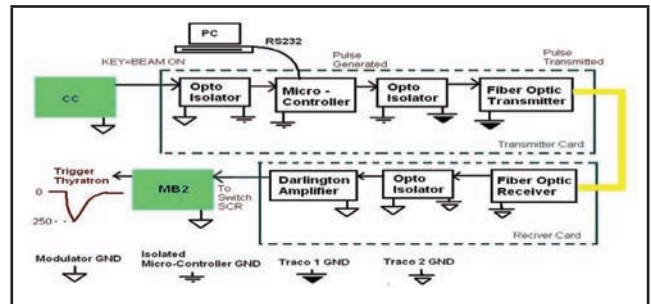


FIG. 27 BLOCK DIAGRAM OF THE LOW VOLTAGE TRIGGER CIRCUIT WITH FIBER OPTIC ISOLATION



FIG. 28 NOISE AND ITS FFT MONITORED AT THE LOW VOLTAGE TRIGGER PULSE WITH FIBER OPTIC ISOLATION IMPLETED.

6.0 CONCLUSION

A high voltage power supply has been designed for providing biasing pulse to high-power Klystron that acts as a RF source to a high energy linear accelerator. The design of discharge section with the specifications of Klystron is presented.

It was a challenge to understand the generation and propagation of unwanted noise frequencies that were hindering the reliable operation of the supply. A thorough investigation is done and most of the noise sources are mapped and the noise from these sources is measured with a reliable measurement technique. The complete analysis of this data is done and compared with a standard regulatory test. In conclusion this study helped us to understand the design considerations that are to be made for reliable operation of such high voltage pulse power supply. The implemented modifications in the system helped to immunize the low voltage control systems from the wide band noise and further designs are being revised for much better noise free operation of the pulse generator.

ACKNOWLEDGEMENT

The authors would like to thank Sandesh R. Bhat, Scientist-C for his assistance in data acquisition and Sagar Sonavane, GAT for his valuable assistance in developing GUIs in LabVIEW. This work is carried out as a core development project sponsored by Department of Electronics & Information Technology (DIETY), India and thanks to Director General, SAMEER for valuable support.

REFERENCES

- [1] C. Mansson, "Pulsed Power Technology and Applications-Scandinavia," TR-112566 Final Report, April 1999.
- [2] S T Pai, Qi Zhang, "Introduction to High Power Pulse Technology" World Scientific Publishing Co Pte Ltd July 31, 1995.
- [3] L.W.Turner, "Electronics Engineer's Reference book," Butterworth & Co.(publishers) Ltd, London:88, Page 7-57
- [4] Maged E.A. Mohamed and Ayman H. AmerEissa, "Pulse Electric fields for Food processing Technology," ch-11, 2004. <http://dx.doi.org/10.5772/48678>
- [5] S.Inoue, S.iizasa, D.Wang, T.Namhihira, M.Shigeishi, M.htsu, H.Akiyama, "Concrete recycling by pulsed power discount" International Journal of Plasma Environmental Science & Technology, Vol.6, No.2, September 2012.
- [6] Roy A, Menon R., Mitra S, Kumar S, Sharma V, Sharma A, Nagesh K.V, Chakravorthy D.P, "High power microwave generation from KALI 5000 pulse power system", IEEE Pulsed Power Conference -2011, Chicago, pp. 387-390, 2011.
- [7] Archana Sharma, Senthil Kumar et. al., "Development and Characterization of Repetitive 1-kJ Marx - Generator-Driven Reflex Triode System for High - Power Microwave Generation," IEEE Trans. Plasma Sci. 39, 2011: 1262 - 1267, 2011.
- [8] Bailey M.R., Cleveland R.O., Colonius T., Crum L.A, Evan A.P., Lingeman J.E., McAteer J.A., Sapozhnikov O.A., Williams J.C. "Cavitation in shock wave lithotripsy: the critical role of bubble activity in stone breakage and kidney trauma "IEEE Symposium on Ultrasonics, Vol 1, pp. 724 - 727, Oct 2003
- [9] Shukla, S.K.Sharma, P.Banerjee, R.Das, P.Deb, B.K. Das, B.Adhikary and A.Shyam, "Low voltage operation of plasma focus" Review of Scientific Instruments. 81, Vol No 8, 2010.
- [10] S K Sharma, SC Jakhar, R Shukla, CVS Rao and A Shyam "Explosive detection system using pulsed 14 MeV neutron source", Fusion Engineering and Design, Vol. 85, pp 1562-1564 Nov 2010.
- [11] P.R. Chalise, S. Perni, G. Shama, B. Novac, I.R. Smith and M.G. Kong, "Lethality Mechanisms in Escherichia coli Induced by Intense Sub-microsecond Electrical Pulses", Appl. Phys. Lett., Vol. 89, pp. 153-902, 2006.
- [12] Akira Mizuno, Yuji Hori, "Destruction of living cells by pulsed high voltage application," IEEE Trans. on Industry Applications, Vol. 24, pp. 387-394, 1988.

- [13] Y. Sun, P.T. Vernier, M. Behrend, L. Marcu and M.A. Gundersen, "Electrode Microchamber for Non-Invasive Perturbation of Mammalian Cells with Nanosecond Pulsed Electric Fields," *IEEE Transactions on Nanobioscience*, Vol. 4, No. 4, pp. 277-283, Dec 2005.
- [14] S. J. Beebe, P. M. Fox, L. J. Rec, K. Somers, R. H. Stark, and K. H. Schoenbach, "Nanosecond pulsed electric field (nsPEF) effects on cells and tissues: apoptosis induction and tumor growth inhibition." *IEEE Trans. Plasma Sci.*, 30:286-292, 2002.
- [15] R. Avakian, A. Avetisyan, R. Dallakyan, I. Kerobyan, "99mTc Photo-Production under Electron Linear Accelerator Beam", *Armenian Journal of Physics*, Vol. 6, No. 1, pp. 35-44, 2013.
- [16] C.J.Karzmark, Craig S.Nunan and Eiji Tanabe, "Medical Electron Accelerators", McGraw Hill, Inc, Newyork,1976.
- [17] P. W. Smith, "Pulsed Power for Particle Accelerators," The CERN Accelerator School, May 12th- 18th, 2004
- [18] G.N.Galsole, J.V.Lebacoz, "Pulse Generators", McGraw Hill Book Company, Inc, Newyork and London.
- [19] Thakur Kiran ,Pethe S N, Krishnan R, "Development of pulse Modulator to Drive 6.19 MW klystron for 15MeV Linac". XXVI th International Symposium on Discharge and Electrical Insulation in vacuum, Mumbai, India -2014 (ISDEIV-2014) 28 Sept - 3 Oct 2014
- [20] F. Artech, B. Allongue, F. Szoncs, C. Rivetta, "EMI Filter Design and Stability Assessment of DC Voltage Distribution based on Switching Converters" 7th Workshop on Electronics for LHC Experiments, Stockholm, Sweden, Sep 2001, pp.353-357.
- [21] C.R. Paul, Introduction to Electromagnetic Compatibility, 2nd Edition, J. Wiley, 2006.
- [22] C. Kondo, T. Inagaki, K. Shirasawa, T. Sakurai, T. Shintake, "EMI noise suppression in the klystron pulse power supply for XFEL/spring-8" Proceedings of IPAC 2010, Kyoto, Japan
- [23] TAO Xiao2Ping, "Analysis of Discharging Noise of Line2Type Pulse Modulator", *High Energy Physics And Nuclear Physics*, Vol. 26 , No. 6 2 June, 2002
- [24] B Burke, M Lamey, S Rathee, B Murray and B G Fallone1, "Radio frequency noise from clinical linear accelerators," *Physics In Medicine And Biology*, 54 (2009) 2483–2492
- [25] 3-Phase+Neutral Line Filters, June 2006, Schaffner<www.schaffner.com>
- [26] Three-Phase Filters for chassis mounting, 690-342F, BenteliHallwag/October 1998© 1997 SchaffnerElektronik<www.schaffner.com>, pp.16-17.